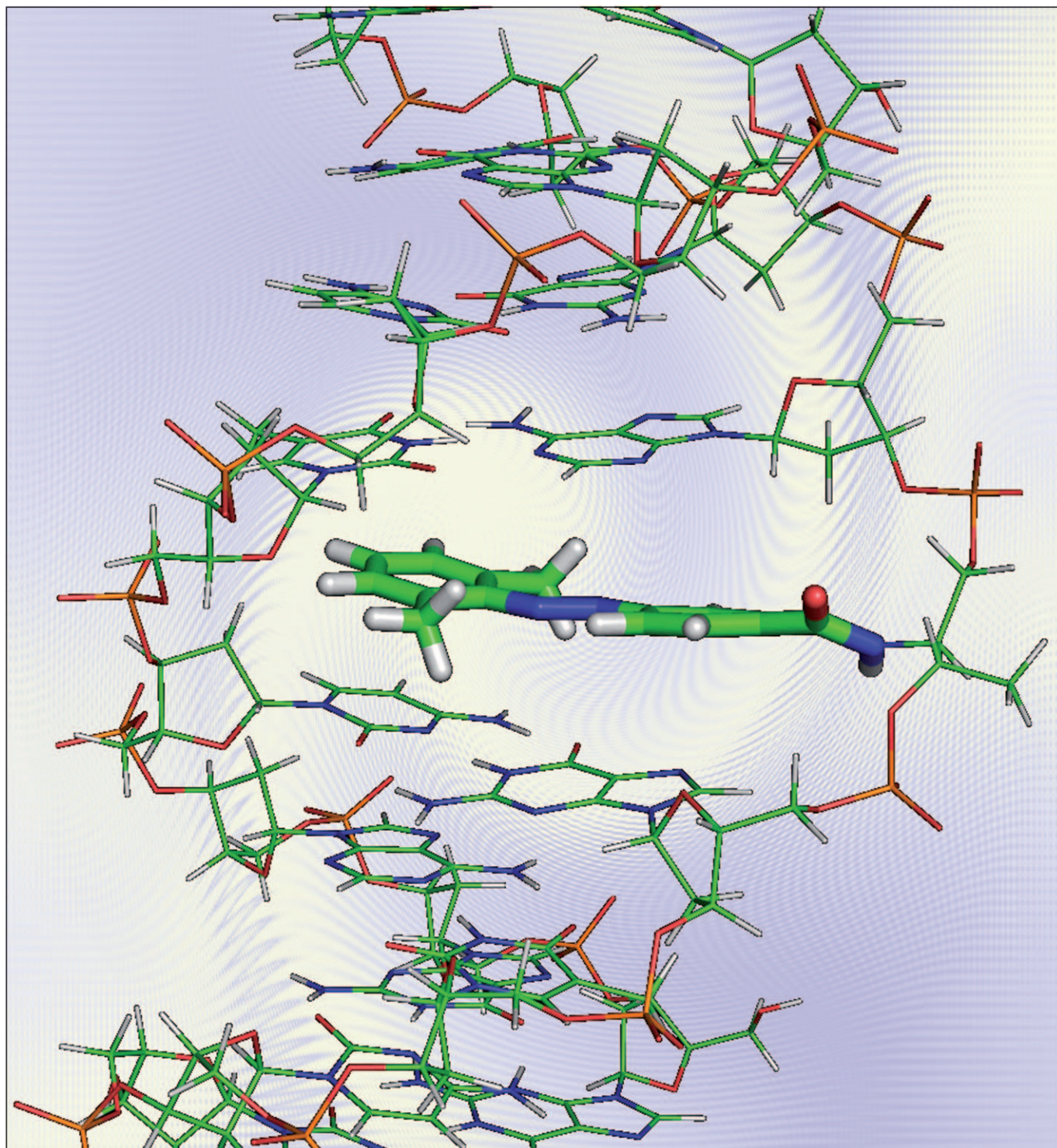


Effect of the *ortho* Modification of Azobenzene on the Photoregulatory Efficiency of DNA Hybridization and the Thermal Stability of its *cis* Form

Hidenori Nishioka,^[a] Xingguo Liang,^{*,[a]} and Hiroyuki Asanuma^{*,[a, b]}



Abstract: We synthesized various azobenzenes methylated at their *ortho* positions with respect to the azo bond for more effective photoregulation of DNA hybridization. Photoregulatory efficiency, evaluated from the change of T_m (ΔT_m) induced by *trans*–*cis* isomerization, was significantly improved for all *ortho*-modified azobenzenes compared with non-modified azobenzene due to the more stabilized *trans* form and the more destabilized *cis* form. Among the synthesized azobenzenes, 4-carboxy-2',6'-dimethylazobenzene (**2',6'-Me-Azo**), in which two *ortho* positions of the distal benzene ring with respect to carboxyl group were methylated, exhibited the largest

ΔT_m , whereas the newly synthesized **2,6-Me-Azo** (4-carboxy-2,6-dimethylazobenzene), which possesses two methyl groups on the two *ortho* positions of the other benzene ring, showed moderate improvement of ΔT_m . Both NMR spectroscopic analysis and computer modeling revealed that the two methyl groups on **2',6'-Me-Azo** were located near the imino protons of adjacent base pairs; these stabilized the DNA duplex by stacking interactions in the *trans* form and destabilized the

Keywords: DNA • intercalations • isomerization • modified azobenzenes • photoswitches

DNA duplex by steric hindrance in the *cis* form. In addition, the thermal stability of *cis*-**2',6'-Me-Azo** was also greatly improved, but not that of *cis*-**2,6-Me-Azo**. Solvent effects on the half-life of the *cis* form demonstrated that *cis*-to-*trans* isomerization of all the modified azobenzenes proceeded through an inversion route. Improved thermal stability of **2',6'-Me-Azo** but not **2,6-Me-Azo** in the *cis* form was attributed to the retardation of the inversion process due to steric hindrance between lone pair electrons of the π orbital of the nitrogen atom and the methyl group on the distal benzene ring.

Introduction

Recently, DNA has come to be regarded not only as a carrier of genetic information but also as an excellent nanomaterial that can perform mechanical motions and construct static nanostructures in a predetermined fashion due to its simple hybridization rule.^[1] However, because achievable performance is still limited by only four natural nucleotides, a variety of functional DNAs involving non-natural molecules have been proposed.^[2] We have developed photoresponsive DNAs involving azobenzenes on acyclic threoninols as scaffolds, and the key feature of DNA, the formation and dissociation of DNA duplexes, can be efficiently photoregulated to create a photon-driven nanomachine as well as photoswitching of enzymatic reactions.^[3]

Among reversible photoswitching molecules, we have been particularly interested in azobenzenes as a photoswitch of DNA for the following reasons: 1) Photoisomerization induces planar/nonplanar structural changes that crucially affect duplex stability;^[4] 2) unlike other photoresponsive molecules, such as spiropyran,^[5] azobenzenes are sufficiently stable in water that repeated photoirradiation does not

cause deterioration or unfavorable chemical reactions; and 3) facile synthetic procedures allow a variety of modifications of azobenzene that can diversify the photoswitching properties.^[6] In fact, we found that even simple alkylation greatly improves the photoregulatory efficiency of DNA hybridization. Modification at the *ortho* position with respect to the N=N bond stabilizes the duplex in the *trans* form, whereas the *cis* form is destabilized compared with the non-modified azobenzene.^[7] As a result, the ΔT_m (the change in melting temperature, T_m) induced by *trans*–*cis* isomerization is significantly enhanced. This improvement was successful only at the *ortho* position, and modification at the *para* position destabilized the duplex even in the *trans* form.^[8] Significantly, methylation at the two *ortho* positions of the distal benzene ring of azobenzene (4-carboxy-2',6'-dimethylazobenzene, **2',6'-Me-Azo**, see Figure 1 for the structure) increased ΔT_m by three-fold compared with the nonmodified

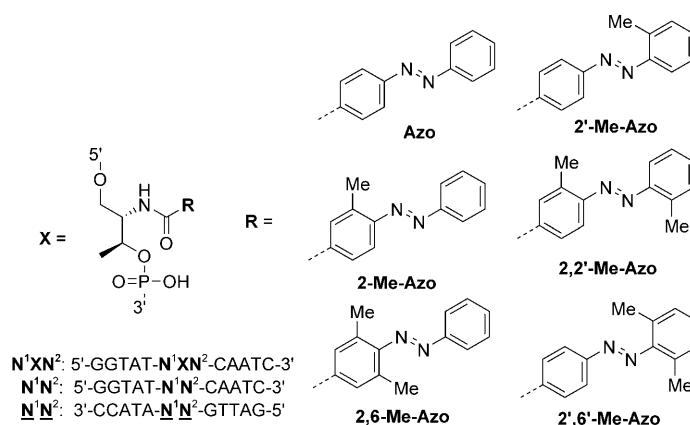


Figure 1. Structures of *ortho*-methylated azobenzenes and the DNA sequences used in this study. N^1 and N^2 represent natural nucleotides (A, G, C, T), and N^1 and N^2 represent their complementary ones. X indicates azobenzene and its derivatives.

[a] H. Nishioka, Prof. Dr. X. G. Liang, Prof. Dr. H. Asanuma
Graduate School of Engineering, Nagoya University
Furo-cho, Chikusa-ku
Nagoya 464-8603 (Japan)
Fax: (+81) 52-789-2528
E-mail: asanuma@mol.nagoya-u.ac.jp
liang@mol.nagoya-u.ac.jp

[b] Prof. Dr. H. Asanuma
Core Research for Evolution Science and Technology (CREST)
(Japan) Science and Technology Agency (JST),
Kawaguchi, Saitama 332-0012 (Japan)

Supporting information for this article is available on the WWW under <http://dx.doi.org/10.1002/chem.200902789>.

form. In addition, we unexpectedly discovered that the *cis* form of **2',6'-Me-Azo** has excellent thermal stability, with a half-life about 10-fold longer than that of nonsubstituted azobenzene (**Azo**).^[7]

Although numerous *ortho*-modified azobenzenes have been synthesized to date,^[9] there have been few reports on improved thermal stability of the *cis* form.^[10]

We investigated in detail the effect of modification of azobenzene at the *ortho* position to improve the photoregulatory efficiency (ΔT_m) of DNA hybridization, as well as the thermal stability of the *cis* form. Because azobenzenes are widely used for photoregulation of various biomolecules and materials,^[11] our analysis potentially improves these applications and clarifies the mechanism of photo- and thermal isomerization that is still in dispute.^[12]

Results

Effect of the position of methylation on photoregulatory efficiency: Structures of *ortho*-substituted azobenzene derivatives are shown in Figure 1, together with the sequences that were evaluated for T_m . We synthesized all possible azobenzenes mono- and dimethylated at the *ortho* positions with respect to the N=N bond.^[13] As listed in Table 1, all modifications of azobenzene in the **CXG/GC** duplex improved the

Table 1. Effect of different alkyl groups in azobenzene on the T_m of **CXG/GC** in the *trans* and *cis* forms.

	T_m [°C] ^[a]		ΔT_m ^[b]
	<i>trans</i>	<i>cis</i>	
Azo	48.9	43.2	5.7
2-Me-Azo	48.8	39.3	9.5
2'-Me-Azo	50.7	40.1	10.6
2,2'-Me-Azo	51.4	39.9	11.5
2,6-Me-Azo	48.6	40.0	8.6
2',6'-Me-Azo	50.9	36.3	14.6

[a] Solution conditions: [DNA]=5 μ M, [NaCl]=100 mM, pH 7.0 (10 mM phosphate buffer). [b] Change in T_m induced by *cis*-*trans* isomerization.

ΔT_m compared with the unmodified **Azo**, mainly due to the decrease in T_m in the *cis* form.^[14] However, the methylated position slightly but distinctly affected the T_m in the *trans* form. For example, **2'-Me-Azo**, in which the distal benzene ring was monomethylated, showed a 2°C higher T_m than **2-Me-Azo**, which was methylated at the proximal ring, whereas the difference in T_m in the *cis* forms was within 1°C. As a result, the ΔT_m of **2'-Me-Azo** was slightly higher than that of **2-Me-Azo**. Similarly, for dimethylated azobenzene the T_m values of **2,2'-Me-Azo** and **2',6'-Me-Azo** were 2–3°C higher than that of **2,6-Me-Azo**, which had no methyl group on the distal benzene ring. For either mono- or disubstitution, modification at the proximal benzene ring only exhibited almost the same T_m as **Azo** (compare **2-Me-Azo** and **2,6-Me-Azo** with **Azo** in Table 1). Thus, modification at the *ortho* position of the distal benzene ring is more effective for stabilizing the duplex in the *trans* form.

Unlike the *trans* form, all the *ortho*-methylated azobenzenes had somewhat lower T_m values in the *cis* form and showed almost the same T_m (around 40°C) except for **2',6'-Me-Azo**. Interestingly, introduction of methyl groups at two *ortho* positions of the distal benzene ring greatly lowered the T_m to as low as 36.3°C, which is 7°C lower than that of *cis*-**Azo**. However, such a large drop in T_m was not observed for **2,6-Me-Azo** methylated at the two *ortho* positions of the proximal benzene ring. Thus, of the *ortho* substituents we examined, **2',6'-Me-Azo** showed the largest ΔT_m , which was three times as large as that of nonmodified **Azo** due to more stabilization in the *trans* form and more destabilization in the *cis* form.

Dependency of the T_m of the duplex involving 2',6'-Me-Azo on DNA sequence: Because the stabilizing effect of the intercalator generally depends on the neighboring base pairs,^[15] we examined the sequence dependence of the T_m of **2',6'-Me-Azo**, which exhibited maximum photoregulatory efficiency, in **CXG/GC**. Irrespective of the sequence, all duplexes were stabilized in the *trans* form and destabilized in the *cis* form compared with native DNA duplexes without azobenzene (Table 2). In all combinations of neighboring base pairs, the T_m values of the *trans* forms were about 5°C higher than that of native DNA, whereas those of the *cis*

Table 2. Effect of neighboring bases on the T_m values of **N₁XN₂N₃** duplexes involving *trans* and *cis* forms of **2',6'-Me-Azo**.^[a]

Duplex	T_m [°C]			ΔT_m ^[c]
	Native duplex ^[b]	<i>trans</i>	<i>cis</i>	
AXA/TT	36.9	44.1 (+7.2) ^[d]	24.6 (−12.3) ^[d]	19.5
AXC/TG	38.3	41.3 (+3.0)	25.7 (−12.6)	15.6
AXG/TC	41.2	47.1 (+5.9)	30.3 (−10.9)	16.8
AXT/TA	36.8	42.5 (+5.7)	21.1 (−15.7)	21.4
CXA/GT	42.6	47.2 (+4.6)	28.8 (−13.8)	18.4
CXC/GG	43.6	47.8 (+4.2)	28.6 (−15.0)	19.2
CXG/GC	47.7	50.9 (+3.2)	36.3 (−11.4)	14.6
CXT/GA	41.3	46.4 (+5.1)	26.3 (−15.0)	20.1
GXA/CT	41.3	48.0 (+6.7)	29.2 (−12.1)	18.8
GXC/CG	46.1	48.0 (+1.9)	32.8 (−13.3)	15.2
GXG/CC	46.5	50.5 (+4.0)	36.3 (−10.2)	14.2
GXT/CA	42.0	47.7 (+5.7)	28.7 (−13.3)	19.0
TXA/AT	36.9	42.8 (+5.9)	24.8 (−12.1)	18.0
TXC/AG	40.3	42.2 (+1.9)	28.0 (−12.3)	14.2
TXG/AC	43.1	48.0 (+4.9)	31.9 (−11.2)	16.1
TXT/AA	38.3	43.1 (+4.8)	21.9 (−16.4)	21.2

[a] Solution conditions: [DNA]=5 μ M, [NaCl]=100 mM, pH 7.0 (10 mM phosphate buffer). [b] Melting temperature of the corresponding native duplex without X residue. [c] Change in T_m induced by *trans*-to-*cis* isomerization of **2',6'-Me-Azo**. [d] The data in parentheses show the difference in T_m between native duplexes and modified duplexes containing *trans*- or *cis*-**2',6'-Me-Azo**.

forms were 10–15°C lower. As a result, ΔT_m increased by as much as 14–20°C, clearly demonstrating that **2',6'-Me-Azo** is a superior photoregulator of DNA hybridization. Note that ΔT_m of **CXG/GC** with **2',6'-Me-Azo** in Table 2 was as large as 14.6°C, but the ΔT_m of nonmodified **Azo** was only 5.7°C.^[16]

NMR spectroscopic analysis and computer modeling of duplex involving 2',6'-Me-Azo: To better understand the superiority of 2',6'-Me-Azo as a photoregulator, both NMR spectroscopic analysis and computer modeling were performed on the 5'-GCGAXGTCC-3'/3'-CGCTCAGG-5' duplex, in which X represents 2',6'-Me-Azo (see Figure 2a).

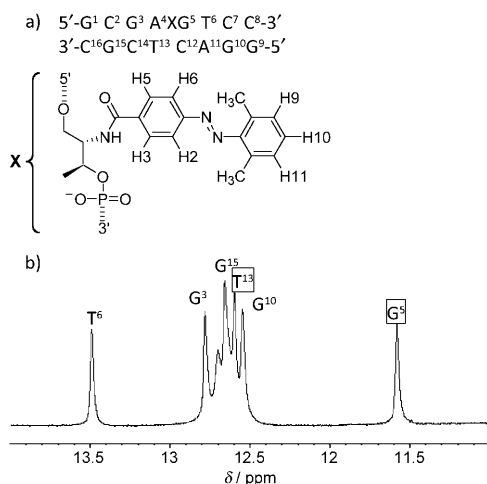


Figure 2. a) Sequence of modified DNAs used for NMR measurements and computer modeling and b) the one-dimensional NMR spectrum at the imino region in H₂O/D₂O (9:1) at 278 K (mixing time = 150 ms), pH 7.0 (20 mM phosphate buffer), in the presence of 200 mM NaCl. The concentration of each DNA was 560 μM. Assignments of the imino protons and the residue numbers are denoted at the top of the peaks.

In trans-2',6'-Me-Azo: First, the position of *trans*-2',6'-Me-Azo in the duplex was determined by NMR spectroscopy. To monitor the imino protons that are exchangeable with water molecules, NMR spectroscopic measurements were carried out in water (H₂O/D₂O 9:1) with a 3-9-19 WATERGATE for H₂O suppression. A one-dimensional spectrum at the region of the imino protons (δ = 11–14 ppm) is depicted in Figure 2b; seven signals corresponding to eight base pairs were exhibited. Except for the terminal G¹ (G¹-C¹⁶ pair) and G⁹ (C⁸-G⁹ pair) that broadened due to rapid exchange with water, all the internal imino protons could be assigned from NOESY, DQF-COSY (double quantum-filtered correlation spectroscopy), and TOCSY (total-correlation spectroscopy).^[17] The signal assigned to G⁵ and T¹³ adjacent to azobenzene (X residue) showed a distinct upfield shift compared with those of G¹⁵, G³, or T⁶ that stayed distant from azobenzene. This upfield shift was attributed to the ring current effect of *trans*-azobenzene, and demonstrates that these protons were located at the axial position.^[18] Figure 3a depicts the NOESY between the imino proton (δ = 11–14 ppm) and the aromatic proton (δ = 5.5–8.0 ppm) regions. Weak NOEs were observed between H⁹ (H¹¹) of the distal ring of 2',6'-Me-Azo, and T¹³ and G⁵ imino protons. In addition, the G⁵ imino proton had relatively strong NOE with the H² (H⁶) aromatic proton on the proximal ring. Methyl protons on 2',6'-Me-Azo also showed distinct NOE with imino protons

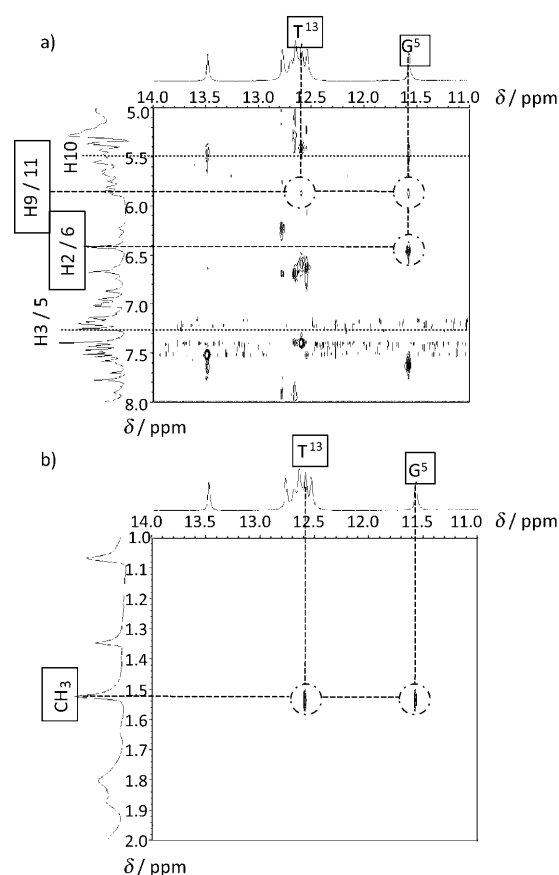


Figure 3. 2D NOESY spectra of the duplex containing *trans*-2',6'-Me-Azo between a) aromatic protons and the imino proton and b) methyl groups and imino proton regions. Solution conditions: [DNA] = 560 μM, [NaCl] = 200 mM, pH 7.0 (20 mM phosphate buffer).

as shown in Figure 3b; strong NOEs were observed for both T¹³ and G⁵ with almost equal intensity. These NOEs clearly demonstrated that 2',6'-Me-Azo is intercalated between A⁴-T¹³ and G⁵-C¹². Computer modeling of this duplex involving *trans*-2',6'-Me-Azo also supported an intercalated structure, as depicted in Figure 4a,b. Two methyl groups of the distal ring were located between the hydrogen-bonded imino protons of G⁵ and T¹³ as depicted in Figure 4b, which was consistent with the NMR spectroscopic results.

In cis-2',6'-Me-Azo: We also measured the NMR spectrum of this duplex in the *cis* form. However, broadened signals assignable to the *cis*-duplex and contaminated sharp peaks of the *trans*-duplex has made the assignment of the NMR signals, even imino proton signals, quite difficult.^[19] Accordingly, structural analysis for the *cis* form was performed only by computer modeling. Because the preliminary analysis indicated that even *cis*-azobenzene is partially intercalated,^[20] we started the calculation with intercalated *cis*-2',6'-Me-Azo as an initial structure. Figure 4c,d shows the converged structure of the duplex with non-planar *cis*-2',6'-Me-Azo, which was located between adjacent base pairs. The proximal benzene ring covalently bound to the main-chain of

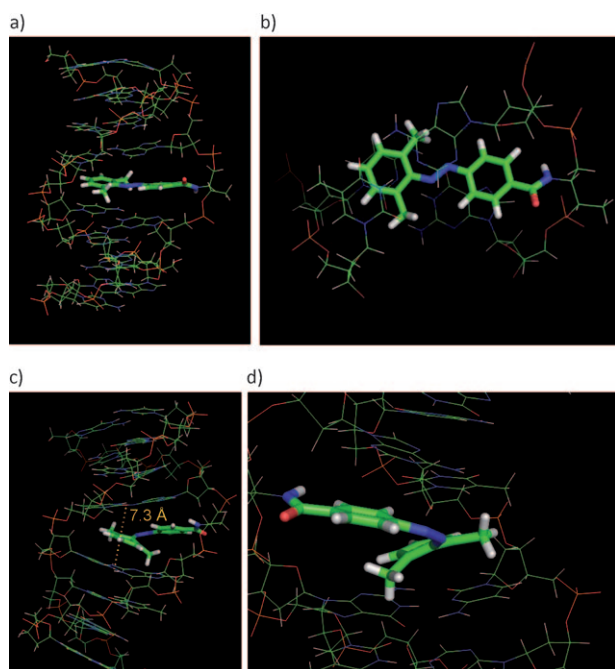


Figure 4. Energy-minimized structure of a modified duplex involving *trans*-2',6'-Me-Azo viewed a) from the side of azobenzene and b) from the 5'-side of the helix axis. For the top view (b), only the 5'-A⁴XG⁵-3'/3'-T¹³C¹²-5' part is depicted and *trans*-2',6'-Me-Azo is drawn in stick form for clarity. c) Whole energy-minimized structure of a modified duplex involving *cis*-2',6'-Me-Azo viewed from the side of azobenzene and d) the same structure magnified around *cis*-2',6'-Me-Azo. The distance between the imino protons of G⁵-C¹² and A⁴-T¹³, depicted with dotted yellow line in (d), was calculated to be 7.3 Å.

threoninol was largely parallel to the A⁴-T¹³ base pair, whereas the distal ring was twisted in the duplex, and the two methyl groups protruded to both adjacent base pairs. As a result, the distance between the imino protons of A⁴-T¹³ and G⁵-C¹² increased to as far as 7.3 Å, resulting in a kink in the duplex at *cis*-2',6'-Me-Azo.

Thermal isomerization of *cis*-azobenzene: To evaluate the thermal stability of the *cis*-azobenzenes, half-lives ($\tau_{1/2}$) of the thermal *cis*-to-*trans* isomerization of the carboxylic acid derivatives were measured in various solvents at 60 °C.^[21] Table 3 shows the half-lives of thermal *cis*-to-*trans* isomerization of these derivatives in the same buffer solution as was used for the T_m measurement and those of the azobenzenes tethered to DNA (CXG) on D-threoninol through an amide bond. As reported previously,^[7] the $\tau_{1/2}$ of 2',6'-Me-Azo tethered to DNA was 25 h, which was about 10 times longer than those of other azobenzenes. We found that newly synthesized 2,6-Me-Azo or 2,2'-Me-Azo, which was methylated on the other two *ortho* positions, did not show such enhanced stability of the *cis* form in DNA. This remarkable effect was observed only when the two *ortho* positions of the distal benzene were methylated. The carboxylic acid form (without DNA) also showed similar results in buffer solution except for 2,6-Me-Azo (not 2',6'-Me-Azo). The $\tau_{1/2}$ of 2,6-Me-Azo in the carboxylic form was 10 h,

Table 3. Half lives ($\tau_{1/2}$) of thermal *cis*-to-*trans* isomerization of azobenzenes in various solvents at 60 °C.^[a]

	Toluene	DMF	Buffer ^[b]
Azo	0.28	1.3	3.4 (3.3) ^[c]
2-Me-Azo	0.34	0.79	3.7 (2.6)
2'-Me-Azo	0.47	1.1	3.5 (3.0)
2,2'-Me-Azo	0.29	0.95	3.3 (2.1)
2,6-Me-Azo	0.14	0.73	10 (2.0)
2',6'-Me-Azo	3.9	9.2	36 (25)

[a] Azobenzene in the carboxylic acid form before introduction into DNA was used for the $\tau_{1/2}$ measurement. [b] [NaCl] = 100 mM, pH 7.0 (10 mM phosphate buffer). [c] The data in parentheses show the $\tau_{1/2}$ of *cis*-azobenzene tethered to single-stranded DNA (CXG) on D-threoninol through an amide bond.

which was five times longer than that tethered to DNA (2.0 h), but still shorter than 2',6'-Me-Azo (36 h). Other azobenzenes had the same or slightly longer $\tau_{1/2}$ compared with those in DNA, indicating that the improved thermal stability of 2',6'-Me-Azo was intrinsic, and not due to the effect of DNA.

We also investigated the effect of the polarity of the solvent on the $\tau_{1/2}$ value to clarify the thermal isomerization pathway. As the polarity of the solvent decreased (water (buffer) → DMF → toluene), the $\tau_{1/2}$ of the *cis* form decreased. For example, the $\tau_{1/2}$ of 2'-Me-Azo was as long as 3.5 h in buffer solution, but only 0.79 h in DMF and 0.47 h in toluene. This solvent effect indicated that thermal isomerization of all the *cis*-azobenzenes proceeds through an inversion mechanism, not a rotation mechanism (vide infra).^[22] 2',6'-Me-Azo also showed the same solvent effect on the $\tau_{1/2}$. Irrespective of the solvent, however, 2',6'-Me-Azo had about a 10-fold longer $\tau_{1/2}$ than other azobenzenes.

Comparison of the activation enthalpy (ΔH^\ddagger) with the activation entropy (ΔS^\ddagger) of the thermal *cis*-to-*trans* isomerization rate further highlighted the uniqueness of 2',6'-Me-Azo (Figure 5). We evaluated ΔH^\ddagger and ΔS^\ddagger of thermal isomerization of all the azobenzenes in single-stranded CXG in buffer solution based on the dependence of thermal isomerization rate on temperature.^[23] As shown in Figure 5, all the

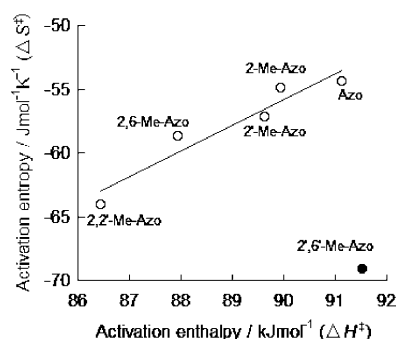


Figure 5. Plot of activation entropy (ΔS^\ddagger) as a function of activation enthalpy (ΔH^\ddagger) at $T=333$ K for the thermal *cis*-to-*trans* isomerization of azobenzenes tethered to single-stranded CXG on D-threoninol in buffer solution.

azobenzenes except for **2',6'-Me-Azo** were aligned almost on the same straight line, demonstrating the typical compensation law of enthalpy and entropy. Interestingly, **2',6'-Me-Azo** deviated greatly from this line, indicating that its thermal isomerization mechanism was different from other azobenzenes.

Discussion

2',6'-Me-Azo as an efficient photoregulator: As shown in Table 1, all the *ortho*-methylated azobenzenes improved photoregulatory efficiency. In particular, **2',6'-Me-Azo** but not **2,6-Me-Azo** showed remarkable improvement due to stabilization of duplex in the *trans* form and destabilization in the *cis* form compared with other azobenzenes, irrespective of the type of adjacent base pairs (see Table 2). For stabilization of the *trans* form by *ortho* modification, methylation at the distal benzene ring, such as in **2'-Me-Azo**, **2,2'-Me-Azo**, and **2',6'-Me-Azo**, was more effective than at the proximal ring. NMR spectroscopic analysis of the duplex with *trans*-**2',6'-Me-Azo** demonstrated that the H2(6) proton at the proximal side had NOE only with imino proton G⁵, whereas both G⁵ and T¹³ had distinct NOE with CH₃ protons; this indicates that the *ortho* positions on the distal side were located on the axial positions of the center of the G⁵-C¹² and A⁴-T¹³ pairs. Consistently, computer modeling also showed that the distal *ortho*-methyl groups were located in close proximity to the adjacent G⁵-C¹² and A⁴-T¹³ pairs, whereas the proximal H2(6) positions were rather distant from these base pairs and located near the *N*-glycosidic linkage between the nucleobase and deoxyribose. We also conducted computer modeling of the duplex containing *trans*-**2,6-Me-Azo** (see Figure S4 of the Supporting Information), and found that two methyl groups were far from the bases. Thus, distal modification at the *ortho* positions made the *trans*-azobenzene a more effective intercalator; this facilitated stacking or hydrophobic interactions between the adjacent base pairs and stabilized the duplex.

On the other hand, destabilization by *cis* isomerization was remarkable only with **2',6'-Me-Azo**. Computer modeling of the duplex with *cis*-**2',6'-Me-Azo** (see Figure 4c,d) revealed that the distal ring was twisted by *cis* isomerization, and the proximal side was fairly parallel to the adjacent A⁴-T¹³ pairs. Because the proximal ring was directly bound to the main chain of threoninol through the rigid amide bond, its orientation might be restricted in the duplex. In contrast, the distal ring was flexible enough to be twisted with respect to the N=N bond by *cis* isomerization. Consequently, the two *ortho* positions protruded close to the base pairs (G⁵-C¹² and A⁴-T¹³) so that they had to be separated to accept the twisted benzene ring with two methyl groups; the distance between the imino protons of G⁵-C¹² and A⁴-T¹³ was calculated to be 7.3 Å as shown with dotted yellow line in Figure 4c; this should significantly hinder their base pairing and thus destabilize the duplex as shown in Figure 4c,d. In the case of *cis*-**2,6-Me-Azo**, computer modeling showed a twist-

ed conformation similar to *cis*-**2',6'-Me-Azo** (see Figure S5 of the Supporting Information). However, the absence of two methyl groups on the twisted distal benzene ring allowed for a smaller space between the G⁵-C¹² and A⁴-T¹³ pairs (the distance was 5.7 Å). Furthermore, because the methyl groups on the proximal ring were far from the bases, steric hindrance might be minimized in the *cis* form. Accordingly, *cis*-**2,6-Me-Azo** less effectively destabilized the duplex than *cis*-**2',6'-Me-Azo**.

Although **2,2'-Me-Azo** involved two methyl groups, free rotation around the C-N bond avoided simultaneous interruption of both G⁵-C¹² and A⁴-T¹³ pairs by forming a proper orientation of these two methyl groups, thus minimizing destabilization.

Unusual thermal stability of *cis*-2',6'-Me-Azo: As summarized in Table 3, **2',6'-Me-Azo** showed unusually slow thermal *cis*-to-*trans* isomerization irrespective of the solvent used. **2,6-Me-Azo**, which possessed two methyl groups on the other benzene ring, did not exhibit improved thermal stability of the *cis* form. Generally, push-pull modifications of azobenzene accelerates thermal isomerization. Because the carboxyl group pulled the electron and the alkyl group weakly pushed it, the *ortho* modification slightly decreased the $\tau_{1/2}$ compared with **Azo** in buffer solution. Furthermore, compensation of ΔH^\ddagger and ΔS^\ddagger indicated that the decreased $\tau_{1/2}$ by *ortho* methylation was caused by a similar electronic effect.^[24] However, *cis*-**2',6'-Me-Azo** exclusively showed different thermal isomerization behavior, as evidenced from the definite deviation in results (see Figure 5).

Asano et al. reported two different routes of thermal *cis*-to-*trans* isomerization: inversion and rotation.^[25] The inversion route proceeds through a transition state in which one of the nitrogen atoms is sp hybridized, whereas the rotation route involves the disruption of a nitrogen-nitrogen π bond and rotation around the remaining σ bond, as shown in Figure 6. These two routes could be discriminated from the $\tau_{1/2}$ dependence on the polarity of the solvent. Because the transition state of the inversion route, an sp-hybridized nitrogen, is stabilized in the apolar solvent due to its hydrophobicity, the $\tau_{1/2}$ decreases as the polarity of the solvent decreases. In contrast, the transition state of the rotation route has a single N-N (not a double N=N) bond that is stabilized in a polar environment, resulting in a smaller $\tau_{1/2}$ with a polar solvent.^[22] The solvent dependence listed in Table 3 clearly demonstrates that the present *ortho*-modified azobenzenes proceeded via an inversion mechanism as the increased polarity of the solvent raised the thermal stability of *cis*-azobenzene.

Nishimura et al. reported on the effect of substituents on the inversion center. They proposed that an electron-accepting substituent enhances the s character of the C-N bond so that an N atom near the electron-accepting substituent becomes the inversion center.^[26] In contrast, an electron-donating substituent allows a distant N atom as the inversion center. According to this hypothesis, an electron-accepting carboxylate group on the distal ring enhances the s charac-

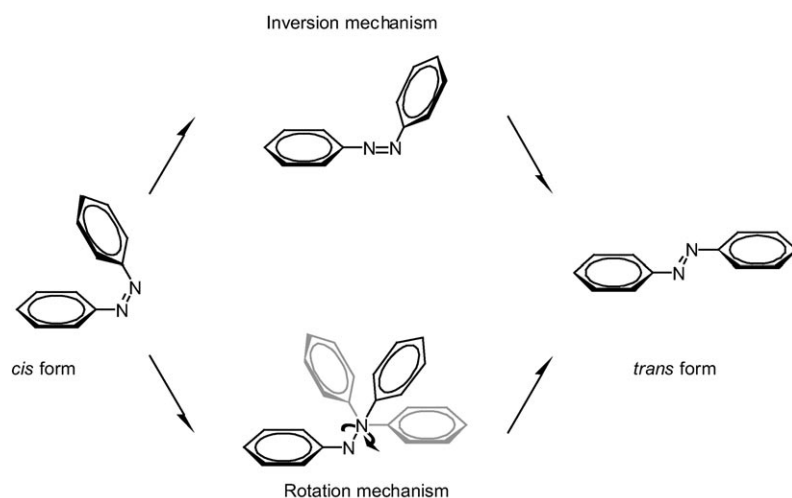


Figure 6. Two possible pathways of *cis*-to-*trans* thermal isomerization. Upper pathway: inversion route through a transition state in which one of the nitrogen atoms is *sp* hybridized. Lower pathway: Rotation route through the rupturing of a nitrogen–nitrogen π bond and rotation around the remaining σ bond.

ter of C–N $_{\alpha}$ (see Figure 7),^[26] which facilitates inversion on the N $_{\alpha}$ atom rather than on N $_{\beta}$. This hypothesis explains the transition states of **2',6'-Me-Azo** and **2,6-Me-Azo** as depicted

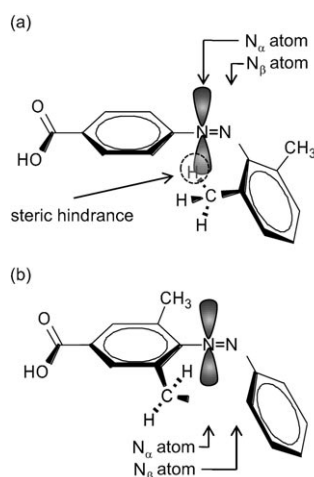


Figure 7. Possible transition states of a) **2',6'-Me-Azo** and b) **2,6-Me-Azo**, both of which have an inversion center at the N $_{\alpha}$ atom. (Sphere-images of transition states of both **2',6'-Me-Azo** and **2,6-Me-Azo** constructed from Insight II/Discover are shown in Figures S6 and S7 of the Supporting Information).

in Figure 7 due to the electron-accepting property of the carboxylic group, thereby leading to the enhanced thermal stability of **2',6'-Me-Azo**. At the transition state, lone pair electrons of the π orbital of the N $_{\alpha}$ atom cause steric hindrance with the methyl groups on the twisted distal benzene ring (see Figure 7a and Figure S6 of the Supporting Information), which could markedly retard the inversion to the *trans* form. However, the two methyl groups on **2,6-Me-Azo** did not induce such steric hindrance with the inversion center of the N $_{\alpha}$ atom (see Figure 7b and Figure S7 of the Supporting In-

formation). Consequently, the *cis*-to-*trans* isomerization of **2,6-Me-Azo** occurred smoothly via an inversion mechanism. In the case of both monosubstituted **2'-Me-Azo** and disubstituted **2',2'-Me-Azo**, this hindrance could be avoided through the smaller hydrogen on other *ortho* position of the distal ring.

In buffer solution, the $\tau_{1/2}$ of **2,6-Me-Azo** in the carboxylic acid form was 5-fold longer than that tethered to DNA (2.0 h), whereas other modified azobenzenes did not elongate the $\tau_{1/2}$ in the carboxylate form. At pH 7, carboxylic acid is mostly deprotonated to form a carboxylate anion thus reducing the electron-accepting property.

In addition, methyl groups on the proximal ring in **2,6-Me-Azo** act as a weak electron donor, which prefers the N $_{\beta}$ atom to the N $_{\alpha}$ atom as an inversion center. Presumably, both the weakened electron-accepting property of the carboxylate anion and the electron-donating methyl groups on the same benzene ring allowed N $_{\beta}$ as well as N $_{\alpha}$ to be inversion centers, and so the thermal isomerization of *cis*-**2,6-Me-Azo** became slower in pH 7 buffer solution. Consistently, the $\tau_{1/2}$ decreased from 10 to 4.8 h when the pH of the solution was lowered from 7 to 5 (see Table S2 of the Supporting Information).^[27]

On the other hand, the $\tau_{1/2}$ of **2',6'-Me-Azo** in the carboxylate form did not depend on the pH; the $\tau_{1/2}$ was as long as 32 h at pH 5.0, which was even longer than that of **2',6'-Me-Azo** tethered to DNA. Although deprotonation of the carboxyl group similarly reduced its electron-donating property, the electron-donating effect of the methyl groups on the distal benzene ring fixed the inversion center at the N $_{\alpha}$ atom even under neutral to basic conditions. In other organic solvents or by conjugation with DNA, however, only the N $_{\alpha}$ atom functioned as an inversion center due to the absence of deprotonation.

Conclusions

We have synthesized various *ortho*-methylated azobenzenes and found that **2',6'-Me-Azo**, in which two methyl groups were introduced to the *ortho* positions of the distal benzene ring, showed the most efficient photoregulatory ability in all combinations of neighboring base pairs. NMR spectroscopic analysis and computer modeling revealed that the two methyl groups located near the adjacent imino protons stabilized the DNA duplex by stacking interactions in the *trans* form and destabilized the DNA duplex by steric hindrance in the *cis* form. The solvent effect on the $\tau_{1/2}$ indicated that

cis-to-*trans* isomerization of all the modified azobenzenes proceeded through an inversion mechanism. The improved thermal stability of the *cis* form of **2',6'-Me-Azo** but not **2,6-Me-Azo** was attributed to steric hindrance between the unpaired electrons of the π orbital of the N atom of the inversion center and the methyl group on the distal benzene ring. By using the present **2',6'-Me-Azo** as a "photon-engine", a photon-driven DNA nanomachine and photoregulation of bioreaction with high "light-fuel cost" can be expected.^[3a,c]

Generally, a push-pull (or push-push) modification of azobenzene shifts the absorption maximum to the visible region ($\lambda > 400$ nm) and allows potential *trans*-to-*cis* isomerization with visible light irradiation. However, if thermal *cis*-to-*trans* isomerization is too fast, these azobenzenes cannot be used practically. Our findings might lead to new modifications of azobenzene that do not accelerate thermal isomerization.

Experimental Section

Materials: Mesitylene, fuming nitric acid, absolute ethanol, and chromic acid were purchased from Kishida Chemical Co. (Osaka, Japan). Nitrosobenzene, 4,4-dimethoxytrityl chloride, and 2-methyl aniline were purchased from Tokyo Chemical Industry (Tokyo, Japan). D-Threoninol was purchased from Sigma-Aldrich (St. Louis, MO, U.S.A.). 2-Cyanoethyl *N,N,N',N'*-tetraisopropylphosphordiamidite was purchased from Chem-Genes (Wilmington, MA, U.S.A.).

Synthesis of DNA involving modified azobenzenes: Modified DNAs containing modified azobenzenes were synthesized by using an automated DNA synthesizer (ABI-3400, Applied Biosystems) from conventional and azobenzene-carrying phosphoramidite monomers. The modified azobenzenes, **2-Me-Azo**, **2'-Me-Azo**, and **2',6'-Me-Azo**, were synthesized and converted to the corresponding phosphoramidite monomers according to a previous report.^[7] Other modified azobenzenes, **2,6-Me-Azo** and **2,2'-Me-Azo**, were synthesized and converted to phosphoramidite monomers as described in the Supporting Information (Schemes S1–3). All modified DNAs were purified by reversed-phase HPLC and characterized by MALDI-TOFMS (Autoflex Linear, Bruker Daltonics). DNAs containing only native bases were supplied by Integrated DNA Technologies (Coralville, IA, U.S.A.).

MALDI-TOF MS for CXG with Azo=X: *m/z* calcd for protonated form: 4020; found: 4021; **2'-Me-Azo=X:** *m/z* calcd: 4034; found: 4035; **2-Me-Azo=X:** *m/z* calcd: 4034; found: 4032; **2,6-Me-Azo=X:** *m/z* calcd: 4048; found: 4047; **2,2'-Me-Azo=X:** *m/z* calcd: 4048; found: 4048; **2',6'-Me-Azo=X:** *m/z* calcd: 4048; found: 4048.

MALDI-TOF MS for DNA containing 2',6'-Me-Azo=X: AXA: *m/z* calcd for protonated form: 4056; found: 4057; **AXC:** *m/z* calcd: 4032; found: 4034; **AXG:** *m/z* calcd: 4072; found: 4072; **AXT:** *m/z* calcd: 4047; found: 4048; **CXA:** *m/z* calcd: 4032; found: 4031; **CXC:** *m/z* calcd: 4008; found: 4009; **CXG:** *m/z* calcd: 4048; found: 4049; **CXT:** *m/z* calcd: 4023; found: 4021; **GXA:** *m/z* calcd: 4072; found: 4070; **GXC:** *m/z* calcd: 4048; found: 4050; **GXG:** *m/z* calcd: 4088; found: 4091; **GXT:** *m/z* calcd: 4063; found: 4062; **TXA:** *m/z* calcd: 4047; found: 4051; **TXC:** *m/z* calcd: 4023; found: 4023; **TXG:** *m/z* calcd: 4063; found: 4063; **TXT:** *m/z* calcd: 4038; found: 4037; 5'-GCGAXGTCC-3' (used for NMR analysis): *m/z* calcd for protonated form: 2814; found: 2814.

T_m measurements: T_m values were determined from the maximum in the first derivative of the melting curve, which was obtained by measuring the absorbance at $\lambda = 260$ nm as a function of temperature. The temperature ramp was $1.0^\circ\text{C min}^{-1}$. Both the heating and cooling curves were measured, and obtained T_m values agreed within 2.0°C . Conditions of the sample solutions: [NaCl] = 100 mM, pH 7.0 (10 mM phosphate buffer), [DNA] = 5 μM .

Photoisomerization of azobenzene: The light source for photo-irradiation was a 150 W Xenon lamp. For the *trans*-to-*cis* isomerization, a UV-D36C filter (Asahi Tech.) was used, and UV light ($\lambda = 300\text{--}400$ nm; 5.3 mW cm^{-2}) was used to irradiate the duplex solution at 60°C for 5 min. Using this procedure, 70–80% of the total azobenzene was isomerized to the *cis* form for all azobenzene derivatives except for **2,6-Me-Azo** and **2',6'-Me-Azo**, in which about 60% was isomerized to the *cis* form. The *cis*-to-*trans* isomerization was carried out by irradiation with visible light ($\lambda > 400$ nm) through an L-42 filter (Asahi Tech.) at 60°C for 5 min. In both cases, a water filter was used to cut off infrared light.

Half-life measurement of thermal isomerization of *cis*-azobenzene to the *trans* form: UV light ($\lambda = 300\text{--}400$ nm; 5.3 mW cm^{-2}) was used to irradiate a solution of single-stranded DNA containing azobenzene at 60°C for 5 min to isomerize *trans*-azobenzene to the *cis* form. Then the solution was measured by using a JASCO V-530 UV/Vis spectrophotometer equipped with a temperature controller, and spectra were monitored at 60°C at predetermined intervals. Half-lives were obtained from the change in absorption maximum of *trans*-azobenzene ($\lambda \approx 340$ nm). Conditions: [NaCl] = 100 mM, pH 7.0 (10 mM phosphate buffer), [DNAs] = 20 μM . Half-life measurements of modified azobenzenes in the carboxylic acid form (without tethering to DNA) were also carried out in the same manner as that with DNA, except for the concentration of azobenzenes was 60 μM .

Calculation of the activation entropy and enthalpy: ΔS^\ddagger and ΔH^\ddagger were calculated based on the following equation:

$$\Delta H^\ddagger = Ea - RT, \Delta S^\ddagger = R[\ln A - \ln(kT/h) - 1.00]$$

in which Ea is the activation energy of thermal isomerization, A is the frequency factor of thermal isomerization, R is the gas constant, k is the Boltzmann constant, and h is the Planck constant.^[23]

NMR spectroscopic analysis of DNA tethering 2',6'-Me-Azo: NMR spectroscopy samples were prepared by dissolving three-times-lyophilized DNAs to a solution of duplex (560 μM) in $\text{H}_2\text{O}/\text{D}_2\text{O}$ (9:1) containing sodium phosphate (20 mM, pH 7.0). NaCl was added to give a final concentration of 200 mM. NMR spectra were measured by using a Varian INOVA (700 MHz) equipped with triple resonance at a probe temperature of 278 K. Resonance was assigned with the standard method by using a combination of 1D, TOCSY (60 ms of mixing time), DQF-COSY, and NOESY (150 ms of mixing time) experiments. All spectra in the $\text{H}_2\text{O}/\text{D}_2\text{O}$ solution were recorded by using a 3-9-19 WATERGATE pulse sequence for water suppression.

Molecular modeling: The insight II/Discover 98.0 program package was used for molecular modeling to obtain energy-minimized structures by conformation-energy minimization. The azobenzene residue was built up by using a graphical program. The results of the NMR spectroscopic analyses served as a starting point for the modeling. For the analysis, the duplex was prepared by positioning the modified azobenzene in the *trans* or *cis* form between the adjacent base pairs. The effect of water and counterions was simulated by a sigmoidal, distance-dependent, direct function. The B-type duplex was used, and the AMBER force field was used for calculation. Computation was carried out by using a Silicon Graphics O2 workstation with the operating system IRIX64 release 6.5.

Acknowledgements

This work was supported by JSPS Research Fellow (to H.N.), the Core Research for Evolution Science and Technology (CREST), the Japan Science and Technology Agency (JST) (to H.A.) Partial support was provided by a Grant-in-Aid for Scientific Research from the Ministry of Education, Culture, Sports, Science and Technology, Japan (to H.A. and X.L.).

[1] Y. Ito, E. Fukusaki, *J. Mol. Catal. B* **2004**, 28, 155–166, and references therein.

- [2] a) N. A. Grigorenko, C. J. Leumann, *Chem. Eur. J.* **2009**, *15*, 639–645; b) B. Chakraborty, R. Sha, N. C. Seeman, *Proc. Natl. Acad. Sci. USA* **2008**, *105*, 17245–17249; c) D. D. Young, H. Lusic, M. O. Lively, J. A. Yoder, A. Deiters, *ChemBioChem* **2008**, *9*, 2937–2940; d) A. T. Krüger, H. G. Lu, A. H. F. Lee, E. T. Kool, *Acc. Chem. Res.* **2007**, *40*, 141–150; e) G. Mayer, A. Heckel, *Angew. Chem.* **2006**, *118*, 5020–5042; *Angew. Chem. Int. Ed.* **2006**, *45*, 4900–4921; f) C. J. Leumann, *Bioorg. Med. Chem.* **2002**, *10*, 841–854, and references therein.
- [3] a) D. Matsunaga, H. Asanuma, M. Komiyama, *J. Am. Chem. Soc.* **2004**, *126*, 11452–11453; b) H. Asanuma, X. G. Liang, H. Nishioka, D. Matsunaga, M. Liu, M. Komiyama, *Nat. Protoc.* **2007**, *2*, 203–212; c) X. G. Liang, H. Nishioka, Takenaka, H. Asanuma, *ChemBioChem* **2008**, *9*, 702–705; d) H. Kashida, X. G. Liang, H. Asanuma, *Curr. Org. Chem.* **2009**, *13*, 1065–1084, and references therein.
- [4] J. M. Robertson, *J. Chem. Soc.* **1939**, 232–236.
- [5] a) H. Asanuma, K. Shirasuka, T. Yoshida, X. G. Liang, M. Komiyama, *Chem. Lett.* **2001**, 108–109; b) J. Andersson, S. Li, P. Lincoln, J. Andréasson, *J. Am. Chem. Soc.* **2008**, *130*, 11836–11837.
- [6] a) T. Gunnlaugsson, J. M. Kelly, M. Nieuwenhuyzen, A. M. K. O'Brien, *Tetrahedron Lett.* **2003**, *44*, 8571–8575; b) Q. Wang, L. Yi, L. Liu, C. Zhou, Z. Xi, *Tetrahedron Lett.* **2008**, *49*, 5087–5089.
- [7] H. Nishioka, X. G. Liang, H. Kashida, H. Asanuma, *Chem. Commun. (Cambridge)* **2007**, 4354–4356.
- [8] Modification at the *para* position led to the reversed photoswitch with the combination of L-threoninol, see X. G. Liang, N. Takenaka, H. Nishioka, H. Asanuma, *Chem. Asian J.* **2008**, *3*, 553–560.
- [9] a) J. P. Ortruba III, R. G. Weiss, *J. Org. Chem.* **1983**, *48*, 3448–3453; b) N. J. Bunce, G. Ferguson, C. L. Forber, G. J. Stachnyk, *J. Org. Chem.* **1987**, *52*, 394–398.
- [10] M. R. Han, D. Hashizume, M. Hara, *New J. Chem.* **2007**, *31*, 1746–1750.
- [11] a) C. Renner, L. Moroder, *ChemBioChem* **2006**, *7*, 868–878; b) S. Yagai, A. Kitamura, *Chem. Soc. Rev.* **2008**, *37*, 1520–1529, and references therein.
- [12] a) T. Ikegami, N. Kurita, H. Sekino, Y. Ishikawa, *J. Phys. Chem. A* **2003**, *107*, 4555–4562; b) H. Satzger, C. Root, M. Braun, *J. Phys. Chem. A* **2004**, *108*, 6265–6271; c) I. Conti, M. Garavelli, G. Orlandi, *J. Am. Chem. Soc.* **2008**, *130*, 5216–5230.
- [13] We did not synthesize tri- or tetramethylated azobenzenes because of the following reasons: Synthesis of tri- or tetraalkylated azobenzenes at *ortho* positions is rather difficult due to the steric hindrance between the methyl groups on both sides of the benzene rings (C. J. Byrne, D. A. R. Happer, M. P. Hartshorn, H. K. J. Powell, *J. Chem. Soc., Perkin Trans. 1* **1987**, 1649–1653). According to the literature (ref. [9b]), tri- or tetraalkylation at the *ortho* positions makes the *trans*-to-*cis* photoisomerization slower, and accordingly the *cis* content after UV light irradiation becomes much less, which is unfavorable for the efficient photoregulation. In addition, we think that further methylation might not improve the photoregulatory efficiency based on our present finding; modification of the distal benzene ring, but not the proximal one was effective for the significant improvement of photoregulatory efficiency.
- [14] Actual T_m curves were depicted in Figure S1 in the Supporting Information.
- [15] R. E. Holmlin, E. D. A. Stemp, J. K. Barton, *Inorg. Chem.* **1998**, *37*, 29–34.
- [16] Our group previously also investigated the sequence dependency of non-modified **Azo** to obtain the nearest-neighbor parameter (H. Asanuma, D. Matsunaga, M. Komiyama, *Nucleic Acids Symp. Ser.* **2005**, *49*, 283–284). It was found that the duplex involving **Azo** showed almost the same dependency of T_m on the adjacent base pair as that of **2',6'-Me-Azo** in both the *trans* and *cis* forms. In addition, although the length of the present sequence involving **2',6'-Me-Azo** was four bases longer than that of **Azo**, which our group previously used, the ΔT_m of **2',6'-Me-Azo** was higher than that of **Azo** in all the sequences, demonstrating the superiority of **2',6'-Me-Azo** (see the Supporting Information, Figure S2 and Table S1).
- [17] The weak signal at $\delta = 12.7$ ppm was assignable to one of the terminal base pairs (G^1 or G^9). Other terminal imino proton signals might be overlapped with the signal at $\delta = 12.8$ ppm.
- [18] X. G. Liang, H. Asanuma, H. Kashida, A. Takasu, T. Sakamoto, G. Kawai, M. Komiyama, *J. Am. Chem. Soc.* **2003**, *125*, 16408–16415.
- [19] As described above, the DNA duplex that contain *cis*-**2',6'-Me-Azo** was much more unstable than that of *trans* form.
- [20] M. Liu, H. Asanuma, M. Komiyama, *J. Am. Chem. Soc.* **2006**, *128*, 1009–1015.
- [21] Typical UV/Vis spectra of the thermal *cis*-to-*trans* isomerization are depicted in Figure S3 in the Supporting Information.
- [22] a) P. Haberfield, P. M. Block, M. S. Lux, *J. Am. Chem. Soc.* **1975**, *97*, 5804–5806; b) K. Baba, H. Ono, E. Itoh, S. Noda, T. Usui, K. Ishihara, M. Inamo, H. D. Takagi, T. Asano, *Chem. Eur. J.* **2006**, *12*, 5328–5333.
- [23] Z. F. Liu, K. Morigaki, T. Enomoto, K. Hashimoto, A. Fujishima, *J. Phys. Chem.* **1992**, *96*, 1875–1880.
- [24] R. C. Petersen, *J. Org. Chem.* **1964**, *29*, 3133–3135.
- [25] T. Asano, T. Okada, *J. Org. Chem.* **1986**, *51*, 4454–4458.
- [26] N. Nishimura, T. Sueyoshi, H. Yamanaka, E. Imai, S. Yamamoto, S. Hasegawa, *Bull. Chem. Soc. Jpn.* **1976**, *49*, 1381–1387.
- [27] Note that the pK_a of benzoic acid is 4.20, indicating that 14–15% of **2,6-Me-Azo** is protonated at pH 5. Therefore, $\tau_{1/2}$ did not increase to 2 h like that of **2,6-Me-Azo** tethered to DNA. We also tried to measure $\tau_{1/2}$ at pH values lower than 4, the pK_a of benzoic acid. But neither **2',6'-Me-Azo** nor **2,6-Me-Azo** would dissolve at all under stronger acidic conditions.

Received: October 9, 2009

Published online: January 26, 2010